ADVANCES IN ATMOSPHERIC SCIENCES, VOL. 36, AUGUST 2019, 804–810

• **Original Paper** •

A Method for Diagnosing the Secondary Circulation with Saturated Moist Entropy Structure in a Mature Tropical Cyclone

Yiwu HUANG[1,2,3], Yihong DUAN*[1], Johnny C. L. CHAN[4], and Xuwei BAO[5]

[1]*State Key Laboratory of Severe Weather, Chinese Academy of Meteorological Sciences, Beijing* 100081*, China*
[2]*University of Chinese Academy of Science, Beijing* 100049*, China*
[3]*National Meteorological Center, China Meteorological Administration, Beijing* 100081*, China*
[4]*School of Energy and Environment, City University of Hong Kong, Hong Kong* 999077*, China*
[5]*Shanghai Typhoon Institute, China Meteorological Administration, Shanghai* 200030*, China*

(Received 19 March 2019; revised 16 May 2019; accepted 21 May 2019)

ABSTRACT

Under the adiabatic, axisymmetric and steady assumption, a relationship between the saturated moist entropy structure and the secondary circulation in a tropical cyclone (TC) is derived from the continuity equation. It is found that the isentropic surfaces coincide with the streamlines, and the streamfunction can be expressed with saturated moist entropy. The secondary circulation and the saturated moist entropy structure depend on each other. Thus, a method for diagnosing the secondary circulation with the structure of saturated moist entropy is proposed. The method is verified with a simulated intense idealized TC with a highly axisymmetric structure. The diagnosed secondary circulation reproduces well the moist inflow in the boundary layer and the moist updraft in the eyewall. This method facilitates secondary circulation diagnosis in theoretical or mature TCs that satisfy the adiabatic, axisymmetric and steady approximations.

Key words: tropical cyclone, saturated moist entropy structure, secondary circulation, diagnosis method

Citation: Huang, Y. W., Y. H. Duan, J. C. L. Chan, and X. W. Bao, 2019: A method for diagnosing the secondary circulation with saturated moist entropy structure in a mature tropical cyclone. *Adv. Atmos. Sci.*, **36**(8), 804–810, https://doi.org/10.1007/s00376-019-9054-5.

Article Highlights:

- With the steady, adiabatic and axisymmetric assumptions, a method for diagnosing the secondary circulation from entropy is proposed.
- The diagnosis method is simpler than the Sawyer–Eliassen equation.

1. Introduction

A mature tropical cyclone (TC) is a highly axisymmetric convective system, which is usually decomposed into an annular vortex (primary circulation) and an in-up-and-out circulation (secondary circulation) in studies of TC dynamics. To the first order, the primary circulation satisfies gradient wind balance and hydrostatic balance. With this premise, the secondary circulation can be diagnosed from the heat source field and momentum source field in a single equation, which is the well-known Sawyer–Eliassen (SE) equation (Eliassen, 1951). This equation has been applied in many theoretical studies (Willoughby, 1979; Schubert and Hack, 1982; Shapiro and Willoughby, 1982; Holland and Merrill, 1984; Hack and Schubert, 1986; Pendergrass and Willoughby, 2009; Fudeyasu and Wang, 2011; Smith et al., 2018). In the general form of the SE equation, the heat and momentum sources contain diabatic heating, eddy heat flux, friction forcing and eddy momentum flux (Fudeyasu and Wang, 2011). Since the SE equation is linear, the contribution of the heating and momentum forcing to the forced secondary circulation can be diagnosed separately. However, to solve the SE equation, the heat and momentum sources have to be either prescribed (Pendergrass and Willoughby, 2009) or given by the azimuthal mean from a simulation (Fudeyasu and Wang, 2011).

Emanuel proposed a simple steady-state axisymmetric TC model (Emanuel, 1986, 1988, 1995) in which the air was assumed to be slantwise neutral and inviscid above the boundary layer. The axisymmetric, adiabatic and steady-state assumption is generally acceptable for the main circulation above the boundary layer in a mature TC. In Emanuel's model, the axisymmetric structure of the saturated entropy

* Corresponding author: Yihong DUAN
Email: duanyh@cma.gov.cn

(or angular momentum) above the boundary layer was established. With a simple boundary layer model, the vertical velocity at the top of the boundary layer and the mean radial velocity within the boundary layer were also derived. However, the secondary circulation was not completely constructed in Emanuel's model, as the radial and vertical velocities above the boundary layer were not given. This hinders studies on the secondary circulation in the theoretical TC model. To obtain the secondary circulation with the SE equation, one has to retrieve the potential heat distribution from the entropy structure, which would make the calculation a bit fussy.

This study proposes a secondary circulation diagnosis method with saturated entropy structure in a steady-state axisymmetric TC under the adiabatic and inviscid assumptions, in order to facilitate the derivation of the secondary circulation in a theoretical or mature TC. The theoretical derivation of the diagnosis method is given in section 2. In section 3, a simulated idealized TC is used to verify the diagnosis method. The main results are summarized in section 4, along with some discussion.

2. Derivation of the diagnosis method

2.1. *Theory*

Assume that the mature TC is steady, adiabatic and axisymmetric. According to the second law of thermodynamics:

$$\frac{\mathrm{d}S^*}{\mathrm{d}t} = Q\,, \tag{1}$$

where S^* is the saturated moist entropy and Q is the diabatic heat source. For the adiabatic process, $Q = 0$, and S^* is conserved. For an axisymmetric and steady-state system, the partial derivatives with respect to time and azimuthal coordinate are zero. The total derivative can be written

$$\frac{\mathrm{d}}{\mathrm{d}t} = u\frac{\partial}{\partial r} + w\frac{\partial}{\partial z}\,, \tag{2}$$

where u and w are the radial and vertical velocity, respectively. So, Eq. (1) can be written for $Q = 0$,

$$u\frac{\partial S^*}{\partial r} + w\frac{\partial S^*}{\partial z} = 0\,, \tag{3}$$

where r and z are the radius and height. And then, a relationship between u and w can be constructed:

$$\frac{u}{w} = \left(\frac{\partial r}{\partial z}\right)_{S^*}\,. \tag{4}$$

Physically, when the TC circulation is axisymmetric and adiabatic, S^* is conserved and the air moves along the S^* surface. The ratio of u to w equals the slope of the S^* surface. Substituting Eq. (4) into Eq. (2), we have

$$\frac{\mathrm{d}}{\mathrm{d}t} = u\left(\frac{\partial}{\partial r}\right)_{S^*} = w\left(\frac{\partial}{\partial z}\right)_{S^*}\,. \tag{5}$$

The continuity equation can be written as

$$\frac{1}{r}\frac{\partial(ru)}{\partial r} + \frac{\partial w}{\partial z} = -\frac{\mathrm{d}\ln\rho}{\mathrm{d}t}\,, \tag{6}$$

where ρ is the air density. Substituting Eqs. (4) and (5) into Eq. (6),

$$\frac{1}{r}\frac{\partial}{\partial r}\left[rw\left(\frac{\partial r}{\partial z}\right)_{S^*}\right] + \frac{\partial w}{\partial z} = -w\left(\frac{\partial \ln\rho}{\partial z}\right)_{S^*}\,. \tag{7}$$

Dividing Eq. (7) by w, and expanding the first term, we get

$$\frac{\partial}{\partial r}\left(\frac{\partial r}{\partial z}\right)_{S^*} + \frac{\partial \ln(rw)}{\partial r}\left(\frac{\partial r}{\partial z}\right)_{S^*} + \frac{\partial \ln w}{\partial z} = -\left(\frac{\partial \ln\rho}{\partial z}\right)_{S^*}\,. \tag{8}$$

For the left-hand side, we have

$$\frac{\partial}{\partial r}\left(\frac{\partial r}{\partial z}\right)_{S^*} = \left(\frac{\partial}{\partial z}\right)_{S^*}\ln\left(\frac{\partial r}{\partial S^*}\right)_z\,, \tag{9}$$

$$\frac{\partial \ln(rw)}{\partial r}\left(\frac{\partial r}{\partial z}\right)_{S^*} + \frac{\partial \ln w}{\partial z} = \left(\frac{\partial}{\partial z}\right)_{S^*}\ln(rw)\,. \tag{10}$$

The derivations of Eq. (9) and Eq. (10) are shown in Appendix A and B, respectively. Substituting Eq. (9) and (10) into Eq. (8), we have

$$\left(\frac{\partial}{\partial z}\right)_{S^*}\ln\left[\rho rw\left(\frac{\partial r}{\partial S^*}\right)_z\right] = 0\,. \tag{11}$$

This implies that the term inside the square brackets is a constant along an S^* surface. Assuming that

$$\lambda = \rho rw\left(\frac{\partial r}{\partial S^*}\right)_z\,, \tag{12}$$

then λ is a function of S^*, which is constant along the S^* surface,

$$w = \frac{\lambda}{\rho r}\left(\frac{\partial S^*}{\partial r}\right)_z\,, \tag{13}$$

and then

$$u = w\left(\frac{\partial r}{\partial z}\right)_{S^*} = -\frac{\lambda}{\rho r}\left(\frac{\partial S^*}{\partial z}\right)_r\,. \tag{14}$$

Assuming that

$$\Lambda(S^*) = \int_{S_0^*}^{S^*}\lambda\mathrm{d}S^*\,, \tag{15}$$

then S_0^* is the value of an initial S^* surface, e.g., the inner edge of the eyewall, or the axis of the TC. Λ is also constant along the S^* surface. Then, Eqs. (13) and (14) can be written as:

$$w = \frac{1}{\rho r}\frac{\mathrm{d}\Lambda}{\mathrm{d}S^*}\left(\frac{\partial S^*}{\partial r}\right)_z = \frac{1}{\rho r}\frac{\partial \Lambda}{\partial r}\,, \tag{16}$$

$$u = -\frac{1}{\rho r}\frac{\mathrm{d}\Lambda}{\mathrm{d}S^*}\left(\frac{\partial S^*}{\partial z}\right)_r = -\frac{1}{\rho r}\frac{\partial \Lambda}{\partial z}\,. \tag{17}$$

Equations (16) and (17) have the form of a streamfunction. Thus, Λ is a streamfunction in a steady-state, adiabatic and axisymmetric TC, and the S^* surfaces coincide with the

streamlines. All the equations above can be easily changed to isobaric coordinates by simply replacing z and w with p and ω, which are the pressure and the vertical velocity in isobaric coordinates respectively.

With the steady-state, adiabatic and axisymmetric assumption, the radial and vertical components of the secondary circulation in TC can be expressed with a function of saturated moist entropy in simple forms. This indicates that the secondary circulation and the structure of the saturated moist entropy depend on each other. With the structure of saturated moist entropy, it is possible to diagnose the secondary circulation.

2.2. *Specific feature of the theory*

Considering the annular air column between two isentropic surfaces S_1^* and S_2^*, if the air density and vertical velocity, or the product of them (ρw), are horizontally homogeneous, the horizontal integration of Eq. (13) from S_1^* to S_2^* is

$$\rho w\left(r_2^2 - r_1^2\right) = 2\int_{S_1^2}^{S_2^*} \lambda \mathrm{d}S^* = 2\left[\Lambda\left(S_2^*\right) - \Lambda\left(S_1^*\right)\right] = \text{const}\,, \tag{18}$$

where r_1 and r_2 are the radii of the isentropic surfaces S_1^* and S_2^* respectively. For a small piece of the annular air column moving between the two S^* surfaces, its mass is constant when the entrainment effect is ignored:

$$m = \rho\pi\left(r_2^2 - r_1^2\right)H = \text{const}\,, \tag{19}$$

where H is the vertical thickness of the air piece. Multiplying Eq. (18) by π/m, we get

$$\frac{w}{H} = \frac{2\pi\left[\Lambda\left(S_2^*\right) - \Lambda\left(S_1^*\right)\right]}{m} = \text{const}\,. \tag{20}$$

Equations (18) and (20) indicate the relationship between the variation of the vertical velocity and the volume change in vertical and horizontal components. The variation of ρ represents the volume change effect of the air piece during its vertical movement, and the variation of $(r_2^2 - r_1^2)$ and H represent the change of the horizontal area and vertical thickness of the air piece, which are the horizontal and vertical components of the volume change respectively. For an upward moving air piece, the volume expands as a result of pressure decline and latent heating. When the vertical velocity increases, the vertical thickness of the air piece increases, and then the horizontal area decreases or its expansion is partly cancelled. The physics is that the vertical acceleration (deceleration) leads to a vertical stretching (compression), which would affect the horizontal area when accompanying a volume change. On the other hand, when the variation of the horizontal area is constrained under some kind of dynamical balance (e.g., the slope of S^* surfaces is constrained by the thermal wind balance in Emanuel's theoretical TC model), then the variation of vertical velocity is controlled by the volume change, which is determined by the gas state equation. The relationship between vertical velocity and horizontal area comes from the constraint of the continuity equation.

2.3. *Physical meaning of λ and Λ*

Equation (12) can be written as

$$\lambda = \frac{1}{2\pi}\rho w\left[\frac{\partial(\pi r^2)}{\partial S^*}\right]_z\,. \tag{21}$$

In cylindrical coordinates, $[\partial(\pi r^2)/\partial S^*]_z$ means the area between two S^* surfaces with difference of unit S^*. So, $\rho w[\partial(\pi r^2)/\partial S^*]_z$ indicates the mass that passes through the horizontal area between the two S^* surfaces with difference of unit S^* in unit time, and the physical meaning of λ is the passing mass in units of radians.

According to Eq. (15), Λ is the integral of λ from the S_0^* surface to the S^* surface. So, the physical meaning of Λ is that the mass passes through the horizontal area between two surfaces, S^* and S_0^*, in units of time and units of radians.

2.4. *Diagnosis method*

In order to diagnose the secondary circulation of the steady axisymmetric TC, the values of λ have to be computed for each S^* surface using a reference level (e.g., the top of the boundary layer) first:

$$\lambda = \rho_0 r_0 w_0\left(\frac{\partial r}{\partial S^*}\right)_{z_0}\,. \tag{22}$$

The value of w on the reference level is needed here. In a theoretical TC model, this can be closed by inducing a boundary layer model, which can provide the radial profile of the vertical velocity on the top of the boundary layer (Emanuel, 1986; Kepert, 2001; Smith et al., 2018). Since $(\partial r/\partial S^*)_{z_0}$ is the reciprocal of the radial gradient of S^*, the level with low radial gradient of S^* (i.e., the S^* surfaces are almost horizontal) would induce large error to the computation of λ. Besides, the low vertical velocity would make the value of λ very sensitive to asymmetry. Thus, the reference level should avoid the area with low radial gradient of S^* and low vertical velocity on the main channel of the secondary circulation.

When the value of λ is computed on the reference level, the value of S^* is the only clue to finding the value of λ for points on the other levels. Thus, the distribution of S^* on the reference level should be monotonic. The portion with repeated values of S^* on the reference level has to be skipped. The surfaces with the same S^* value but not originated from the reference level also have to be excluded because the corresponding values of λ may be different. Usually, the main channel of the secondary circulation is left after the exclusion. With the distribution of S^* in the r–z plane, the radial and vertical gradient of S^* and the value of λ for each available point can be obtained, then the radial and vertical components of the secondary circulation can be calculated with Eq. (16) and (17).

3. Verification with idealized simulation

To verify the validation of the diagnosis method, a simulated idealized TC on an f-plane is used in this section. The

Weather Research and Forecasting model, version 3.5.1, is used. The profile of the ambient atmosphere is given by the climatic mean of the NCEP reanalysis data over the tropical area of the western North Pacific (6°–20°N, 125°–160°E) in the typhoon season (from June to September). The initial vortex is the same as the one described in Wong and Chan (2004). The idealized TC is simulated in a nested grid with three domains with a resolution of 15, 5 and 1.67 km respectively. WSM6 (Hong et al., 2006) and the Yonsei University PBL scheme (Hong et al., 2006) are employed. The radiation scheme is switched off and no cumulus scheme is used. Since the upward motion is pseudo-adiabatic in the simulated TC and the corresponding conserved quantity is equivalent potential temperature, the structure of equivalent potential temperature is used for diagnosis in this section instead of saturated moist entropy.

The intensity of the idealized TC increases to 95 m s^{-1} and the TC becomes highly axisymmetric after 96 h of integration. The azimuthal mean structure of the equivalent potential temperature (θ_e) in the r–z plane is shown in Fig. 1 (black solid contours), along with the vertical velocity (color fill) and the 95% relative humidity (RH, red dashed contours). The less saturated portion with RH < 95% in the updraft channel implies that dry air may intrude into the updraft and evaporation may happen, or there may be downward motion when computing the azimuthal mean in the updraft channel. The former situation breaks the adiabatic assumption, while the latter breaks the axisymmetric assumption. Therefore, the less saturated portion will be excluded when diagnosing the secondary circulation. This exclusion also helps to exclude the surfaces with the same θ_e value but not originated from the reference level. The level of 2 km is chosen as the reference level. The values of λ within the monotonic portion are calculated. The diagnosed radial and vertical velocities along the main updraft are shown in Fig. 2 and Fig. 3.

In the vertical component (w), there are three peaks in the simulation, and the diagnosed result captures this feature well (Fig. 2a). The relative difference between the diagnosis and the simulation is defined as $dw_{rela} = (w_{diag} - w)/w$ for quantitative validation. The relative differences over the peaks are between −0.2 to 0.2, indicating good estimations (Fig. 2b). There are some large biases at the edge of the updraft. These bias may be caused either by the θ_e surfaces with different origin, which is not excluded completely with RH < 95%, or by the effect of asymmetry on

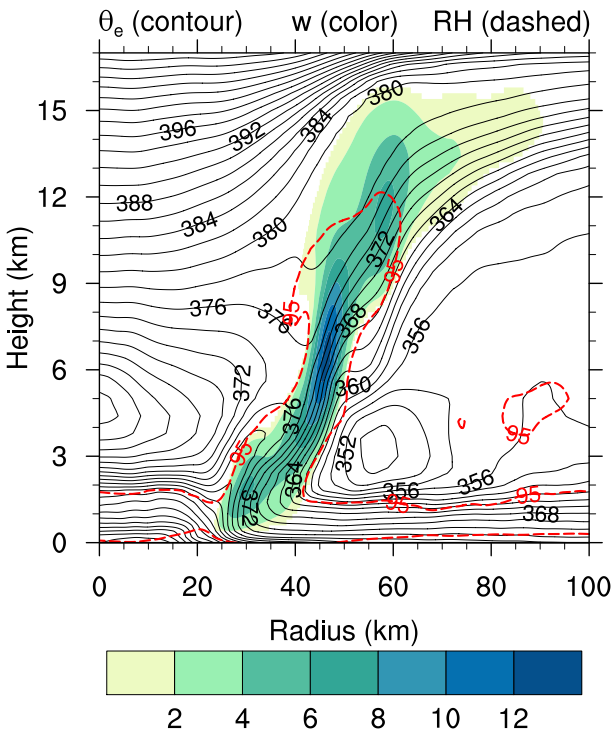

Fig. 1. Azimuthal mean structure of θ_e (units: K; black contours; interval: 2 K) and w (units: m s^{-1}; color fill; interval: 2 m s^{-1}; values < 1 m s^{-1} are not shown) of the simulated ideal TC in the r–z plane. The contour of RH = 95% is also shown (red dashed lines).

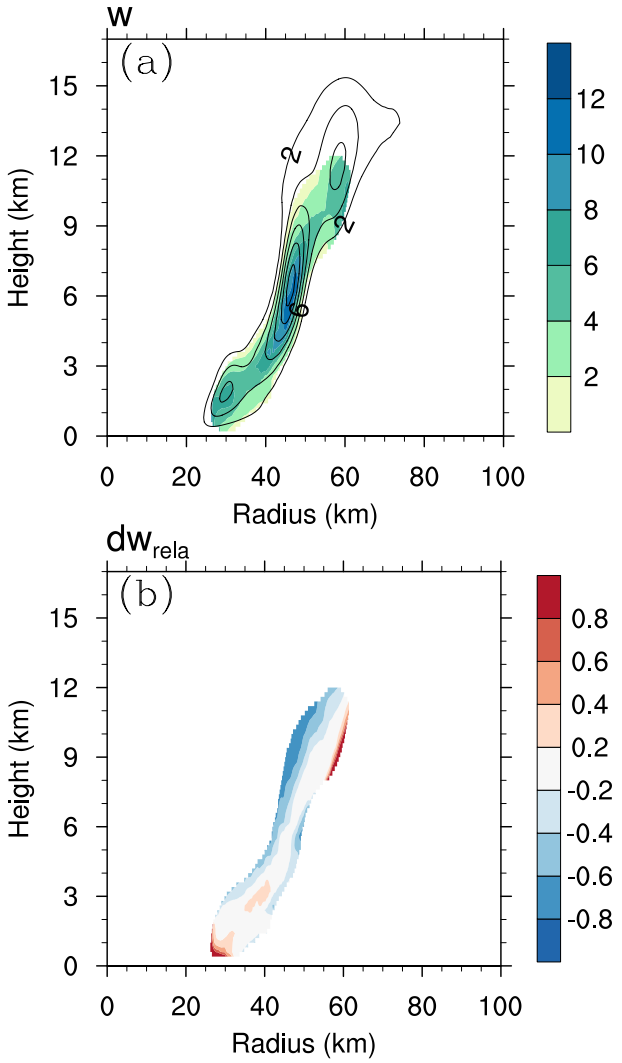

Fig. 2. (a) Simulated (contours; interval: 2 m s^{-1}) and diagnosed (color fill; values < 1 m s^{-1} not shown) vertical velocity (units: m s^{-1}). (b) Relative difference of vertical velocity, $dw_{rela} = (w_{diag} - w)/w$.

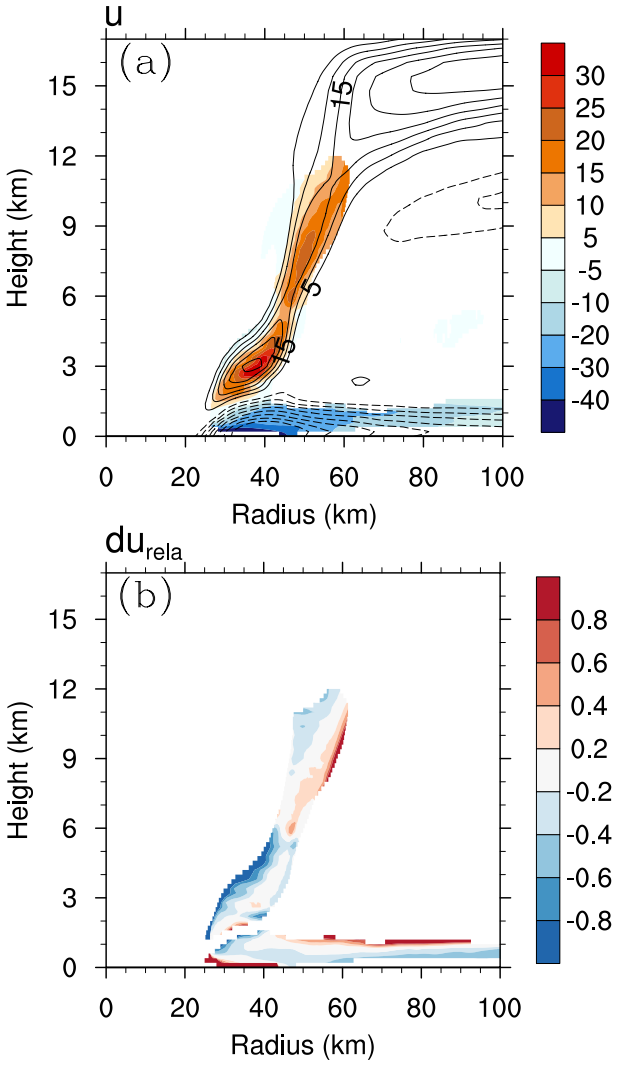

Fig. 3. As in Fig. 2, but for radial velocity (units: m s^{-1}).

the radial gradient of θ_e. Note that there is a drastic variation in the radial gradient of θ_e on the inner edge of the eyewall above 4 km (Fig. 1), which makes the radial gradient of θ_e highly sensitive to the asymmetry of the eyewall radius. This area corresponds well with the large-error area at the upper inner side of the eyewall (Fig. 2b).

There are also three peaks for the simulated positive radial velocity (u) area (Fig. 3a). However, the diagnosis covers only two of them: the mid-level one and the low-level one. Errors are small in the two peak areas, but become large below 6 km on the inner edge of eyewall (Fig. 3b). Unlike the radial gradient of θ_e, the drastic variation in the vertical gradient of θ_e happens in the vicinity where the slopes of the θ_e surfaces turn from vertical to slantwise or from slantwise to vertical, e.g., the inner edge of the eyewall between 1 and 6 km (Fig. 1). Asymmetry in this area could easily induce error to the vertical gradient of θ_e, and then to the diagnosed result. The diagnosed values of u within the boundary layer are also shown. Note that the adiabatic assumption is not fully satisfied since there is a diabatic heat source contributed by sensible heating. However, the inflow is reproduced well by the diagnosis, except that the values are underestimated in the main channel and overestimated on the top and near the surface right below the eyewall.

4. Summary and discussion

With the steady, adiabatic and axisymmetric assumptions, the relationship between saturated moist entropy and secondary circulation is derived from the continuity equation. It is found that the isentropic surfaces coincide with streamlines and the streamfunction can be expressed with entropy. The secondary circulation and the structure of entropy in the r–z plane are dependent on each other. Then, a method for diagnosing the secondary circulation with saturated moist entropy structure in a steady, adiabatic and axisymmetric TC is proposed. With the profile of the vertical velocity on a reference level (e.g., a level slightly higher than the top of the boundary layer), and the structure of saturated moist entropy (or equivalent potential temperature for pseudo-adiabatic assumption) in the r–z plane, the secondary circulation can be diagnosed. The application is shown with a simulated intense idealized TC with a highly axisymmetric structure. Compared with the azimuthal mean of the simulation, the diagnosed result reproduces well the moist inflow within the boundary layer and the moist updraft within the eyewall.

Compared with the SE equation, this diagnosis method is simpler. The prescribed fields needed in the method are density, entropy and vertical velocity on the reference level, which are easy to obtain from simulations and a theoretical TC model (e.g., Emanuel, 1986). Although the prescribed fields on the reference level are limited in the monotonic portion, they cover the main secondary circulation channel in a simulated TC. The limitation is not a problem in a theoretical TC model because the entropy is monotonic at any level above the boundary layer (see Emanuel, 1986). Unlike the SE equation, this diagnosis method does not need preset proper boundary conditions or to satisfy an elliptical discriminant condition (Fudeyasu and Wang, 2011). The thermal wind balance is not necessary for the diagnosis method and the application is valid in the boundary layer. Thus, the method proposed in this study facilitates the diagnosis of the secondary circulation in a simulated mature TC, especially in a theoretical TC model.

This diagnosis method comes from constraint of the continuity equation with adiabatic, axisymmetric, steady-state assumptions. These assumptions are shared in Emanuel's theory (Emanuel, 1986). The dynamics constraining the entropy structure above the boundary layer in Emanuel's theory are the gradient wind balance and the hydrostatic balance, which came from the first order (or zero order in Willoughby, 1979) approximation of the horizontal and vertical momentum equations respectively. However, the constraint of the continuity equation is not introduced in that theory. Emanuel brought in a slantwise neutral assumption to exclude the ambient convective available potential energy, which implied

that the air is neutrally buoyant when ascending along surfaces of constant angular momentum and there is no upward acceleration. However, the vertical velocity should decrease when air parcels approach the top layer of the TC (Camp and Montgomery, 2001). The diagnosis method proposed in this study provides a chance to determine how the dynamic balances constrain the secondary circulation in a theoretical TC model.

Acknowledgements. This article was funded in part by the National Basic Research and Development (973) Program of China (Grant No. 2015CB452805) and in part by the National Natural Science Foundation of China (Grant No. 41775064) and the Basic Research Fund of CAMS (2016Z003). The work of Johnny C. L. CHAN was supported by the Research Grants Council of the Hong Kong Special Administrative Region of China (Grant No. CityU11301417).

APPENDIX A

Derivation of Eq. (9)

$\partial/\partial r$ and $\partial/\partial z$ can be written as $[\partial/(\partial r)]_z$ and $(\partial/\partial z)_r$. The left-hand side of Eq. (9) can transform as below:

$$\left(\frac{\partial}{\partial r}\right)_z\left(\frac{\partial r}{\partial z}\right)_{S^*}=\left(\frac{\partial S^*}{\partial r}\right)_z\left(\frac{\partial}{\partial S^*}\right)_z\left(\frac{\partial r}{\partial z}\right)_{S^*}. \tag{A1}$$

Since

$$\left(\frac{\partial}{\partial S^*}\right)_z\left(\frac{\partial r}{\partial z}\right)_{S^*}=\left(\frac{\partial}{\partial z}\right)_{S^*}\left(\frac{\partial r}{\partial S^*}\right)_z, \tag{A2}$$

and

$$\left(\frac{\partial S^*}{\partial r}\right)_z=\frac{1}{\left(\frac{\partial r}{\partial S^*}\right)_z}, \tag{A3}$$

Eq. (A1) can be written as

$$\left(\frac{\partial}{\partial r}\right)_z\left(\frac{\partial r}{\partial z}\right)_{S^*}=\left(\frac{\partial}{\partial z}\right)_{S^*}\ln\left(\frac{\partial r}{\partial S^*}\right)_z. \tag{A4}$$

APPENDIX B

Derivation of Eq. (10)

Along the r surface, $\ln r$ is constant. So, there is

$$\frac{\partial \ln r}{\partial z}=0. \tag{B1}$$

Adding $\partial \ln w/\partial z$ on both sides, we get

$$\frac{\partial \ln r}{\partial z}+\frac{\partial \ln w}{\partial z}=\frac{\partial \ln w}{\partial z}. \tag{B2}$$

Combining the two terms on the left-hand side gives

$$\frac{\partial \ln(rw)}{\partial z}=\frac{\partial \ln w}{\partial z}. \tag{B3}$$

For a continuously differentiable variable f, there is

$$\frac{\partial f}{\partial r}\left(\frac{\partial r}{\partial z}\right)_{S^*}+\frac{\partial f}{\partial z}=\left(\frac{\partial f}{\partial z}\right)_{S^*}. \tag{B4}$$

When $f=\ln(rw)$, Eq. (B4) can be written as

$$\frac{\partial \ln(rw)}{\partial r}\left(\frac{\partial r}{\partial z}\right)_{S^*}+\frac{\partial \ln(rw)}{\partial z}=\left(\frac{\partial}{\partial z}\right)_{S^*}\ln(rw). \tag{B5}$$

Substituting Eq. (B3) into Eq. (B5),

$$\frac{\partial \ln(rw)}{\partial r}\left(\frac{\partial r}{\partial z}\right)_{S^*}+\frac{\partial \ln w}{\partial z}=\left(\frac{\partial}{\partial z}\right)_{S^*}\ln(rw). \tag{B6}$$

REFERENCES

Camp, J. P., and M. T. Montgomery, 2001: Hurricane maximum intensity: Past and present. *Mon. Wea. Rev.*, **129**, 1704–1717, https://doi.org/10.1175/1520-0493(2001)129<1704:HMIPAP>2.0.CO;2.

Eliassen, A., 1951: Slow thermally or frictionally controlled meridional circulation in a circular vortex. *Astrophisica Norvegica*, **5**, 19–60.

Emanuel, K. A., 1986: An air-sea interaction theory for tropical cyclones. Part I: Steady-state maintenance. *J. Atmos. Sci.*, **43**, 585–605, https://doi.org/10.1175/1520-0469(1986)043<0585:AASITF>2.0.CO;2.

Emanuel, K. A., 1988: The maximum intensity of hurricanes. *J. Atmos. Sci.*, **45**, 1143–1155, https://doi.org/10.1175/1520-0469(1988)045<1143:TMIOH>2.0.CO;2.

Emanuel, K. A., 1995: Sensitivity of tropical cyclones to surface exchange coefficients and a revised steady-state model incorporating eye dynamics. *J. Atmos. Sci.*, **52**, 3969–3976, https://doi.org/10.1175/1520-0469(1995)052<3969:SOTCTS>2.0.CO;2.

Fudeyasu, H., and Y. Q. Wang, 2011: Balanced contribution to the intensification of a tropical cyclone simulated in TCM4: Outer-core spinup process. *J. Atmos. Sci.*, **68**, 430–449, https://doi.org/10.1175/2010JAS3523.1.

Hack, J. J., and W. H. Schubert, 1986: Nonlinear response of atmospheric vortices to heating by organized cumulus convection. *J. Atmos. Sci.*, **43**, 1559–1573, https://doi.org/10.1175/1520-0469(1986)043<1559:NROAVT>2.0.CO;2.

Holland, G. J., and R. T. Merrill, 1984: On the dynamics of tropical cyclone structural changes. *Quart. J. Roy. Meteor. Soc.*, **110**, 723–745, https://doi.org/10.1002/qj.49711046510.

Hong, S. Y., and J. O. J. Lim, 2006: The WRF single-moment 6-class microphysics scheme (WSM6). *Journal of the Korean Meteorological Society*, **42**, 129–151.

Hong, S. Y., Y. Noh, and J. Dudhia, 2006: A new vertical diffusion package with an explicit treatment of entrainment processes. *Mon. Wea. Rev.*, **134**, 2318–2341, https://doi.org/10.1175/MWR3199.1.

Kepert, J., 2001: The Dynamics of Boundary Layer Jets within the Tropical Cyclone Core. Part I: Linear Theory. *J. Atmos. Sci.*, **58**, 2469–2484, https://doi.org/10.1175/1520-0469(2001)058<2469:TDOBLJ>2.0.CO;2.

Pendergrass, A. G., and H. E. Willoughby, 2009: Diabatically induced secondary flows in tropical cyclones. Part I: Quasi-steady forcing. *Mon. Wea. Rev.*, **137**, 805–821, https://doi.org/10.1175/2008MWR2657.1.

Schubert, W. H., and J. J. Hack, 1982: Inertial stability and tropical cyclone development. *J. Atmos. Sci*., **39**, 1687–1697, https://doi.org/10.1175/1520-0469(1982)039<1687:ISATCD>2.0.CO;2.

Shapiro, L. J., and H. E. Willoughby, 1982: The response of balanced hurricanes to local sources of heat and momentum. *J. Atmos. Sci*., **39**, 378–394, https://doi.org/10.1175/1520-0469(1982)039<0378:TROBHT>2.0.CO;2.

Smith, R. K., and M. T. Montgomery, and H. Bui, 2018: Axisymmetric balance dynamics of tropical cyclone intensification and its breakdown revisited. *J. Atmos. Sci*., **75**, 3169–3189, https://doi.org/10.1175/JAS-D-17-0179.1.

Willoughby, H. E., 1979: Forced secondary circulations in hurricanes. *J. Geophys. Res. Oceans*., **84**, 3173–3183, https://doi.org/10.1029/JC084iC06p03173.

Wong, M. L. M., and J. C. L. Chan, 2004: Tropical cyclone intensity in vertical wind shear. *J. Atmos. Sci*., **61**, 1859–1876, https://doi.org/10.1175/1520-0469(2004)061<1859:TCIIVW>2.0.CO;2.